Polymer Chemistry

Accepted Manuscript

This is an *Accepted Manuscript*, which has been through the Royal Society of Chemistry peer review process and has been accepted for publication.

Accepted Manuscripts are published online shortly after acceptance, before technical editing, formatting and proof reading. Using this free service, authors can make their results available to the community, in citable form, before we publish the edited article. We will replace this *Accepted Manuscript* with the edited and formatted *Advance Article* as soon as it is available.

You can find more information about *Accepted Manuscripts* in the Information for Authors.

Please note that technical editing may introduce minor changes to the text and/or graphics, which may alter content. The journal's standard Terms & Conditions and the Ethical guidelines still apply. In no event shall the Royal Society of Chemistry be held responsible for any errors or omissions in this *Accepted Manuscript* or any consequences arising from the use of any information it contains.

ROYAL SOCIETY OF CHEMISTRY

www.rsc.org/polymers

Journal Name

RSCPublishing

ARTICLE

pH-Responsive Dendritic Polyrotaxane drug-polymer conjugates forming nanoparticles as efficient drug delivery system for cancer therapy

Cite this: DOI: 10.1039/x0xx00000x

Received 00th January 2012,
Accepted 00th January 2012

DOI: 10.1039/x0xx00000x

www.rsc.org/

Yang Kang,[a] Xiao-Mei Zhang,[a] Sheng Zhang,[*b] Li-Sheng Ding[a] and Bang-Jing Li[*a]

Self-assembly of stimuli-responsive polymeric nanoparticles have attracted great attention in recent years due to their prospective biological applications. This paper developed a novel pH-sensitive amphiphilic dendritic polyrotaxane drug-polymer conjugate by covalently linked doxorubicin (DOX) and dendritic polyrotaxane via pH-responsible hydrazone bond with 1.84 wt% (weight percent) of DOX. The drug-polymer conjugate that was amphiphilic and could self-assembled to micelles (PR-g-DOX micelles) in aqueous solution. The globular morphology and compact micelles with diameter around 110 nm were observed by SEM and TEM. Meanwhile, the micelles showed a significantly faster DOX release at mildly acidic pH of 6.0 and 5.0 and almost without the burst release at physiological pH of 7.4. Notably, it was confirmed that this micelle could efficiently delivery DOX to the nuclear of the tumor cells, and led to much more cytotoxic effects to A549 cancer cells than parent DOX. In vivo results revealed the better drug tolerability of the PR-g-DOX micelles and a higher in vivo efficacy without increasing its toxicity of the PR-g-DOX micelles. Furthermore, the maximum tolerated dose (MTD) results showed that PR-g-DOX micelles showed an excellent safety profile with a 2-folder MTD (10 mg/kg DOX) than that of free DOX (5 mg/kg DOX). We are convinced that this PR-g-DOX micelle has tremendous potentials for targeted cancer therapy.

Introduction

In the past two decades, stimuli-responsive amphiphilic block copolymers which could self-assembled into different morphologies like micelle or vesicle that are triggered by intracellular signals such as pH, glutathione or specific proteins/enzymes and external factors including heat, light, and ultrasound have attracted more and more attention for applications in various fields such as biomimetics, gene delivery, separation, catalysis, chemical and biological sensing, and drug delivery.[1-17]

Apart from the conventional linear copolymers and well-known spherical symmetry of dendrimers, linear-dendritic copolymers are a unique class of macromolecules with unique solid and solution state properties. They are in very close dependence on the chemistry, size and solvophilicity gradient between the respective blocks and have generated interest for their potential use as drug and gene delivery devices because of their ability to form micelles with critical micelle concentration (CMC) values well below the CMC values of traditional surfactants.[18-20] Among the numerous types of dendritic structures, polyester dendrimers are most attractive due to their because of their biodegradability and nontoxicity, which allows the macromolecules to degrade or hydrolyze into small nontoxic molecules for exclusion from the body rapidly.[21, 22] However, the utility of dendritic polymers is greatly hampered because of the tedious multistep syntheses requiring extensive purifications, and the high generation dendrimer that over five generation can cause side effects due to their slow degradation and preparing a dendrimer that circulate in the blood long enough to accumulate at target tissue is still a great challenge for most of us.[23-25]

Cyclodextrin (CD), one of the promising hosts for macromolecular recognition, has been studied for constructing supramolecular structures and has been found that hierarchical self-assembly via inclusion complexation depends on the complexation behavior of CDs with guest polymer.[26] In recent years, supramolecular assembiles have attracted more and more attention due to their potential to serve as molecular shuttles, motors and machines.[27-32] Among them, CD-based (Pseudo) polyrotaxanes have been extensively studies for their uses as carriers in drug delivery, such as thermo-/pH-sensitive hydrogels,[33-35] vesicles and micelles as carriers for the controlled drug release[36] and gene carriers[37-39]. However, (Pseudo) polyrotaxanes self-assembles from cyclodextrins (CDs) and polyesters were apt to form crystallized precipitate seriously in most of solvent, especially in water, which limited their development in biomedical applications profoundly.

In this article, amphiphilic block copolymers with novel architecture, a pH-sensitive amphiphilic dendritic polyrotaxane

polymer-drug conjugate (PR-g-DOX), were successfully developed through a highly efficient approach. Since this design also renders the hydrophilic property of the dendritic end with eight hydroxyl groups, the hydrophobic property and the π-π interactions of DOX at the linear end, the resulted amphiphilic dendritic polyrotaxane drug-polymer conjugate could form stable micelles (PR-g-DOX micelles) in aqueous solution, which could leads to an accumulation in the cancerous tissues via tumors' enhanced permeability and retention (EPR) effect, and could be triggered to release the DOX by the mildly acidic environment in tumor tissue and at endosomal compartments.[13] Scheme 1 illustrated the formation of PR-g-DOX micelles and the micelles selectively releasing drugs. Herein, the synthesis of dendritic polyrotaxane drug-polymer conjugate, the formation of the micelles, the characteristics of micelles such as size and morphology, zeta potential, and pH-dependent drug release, intracellular release and trafficking of DOX, in vitro drug efficacy and toxicity were investigated. The results demonstrate the promising use of this novel amphiphilic dendritic polyrotaxane drug-polymer conjugate for cancer therapy.

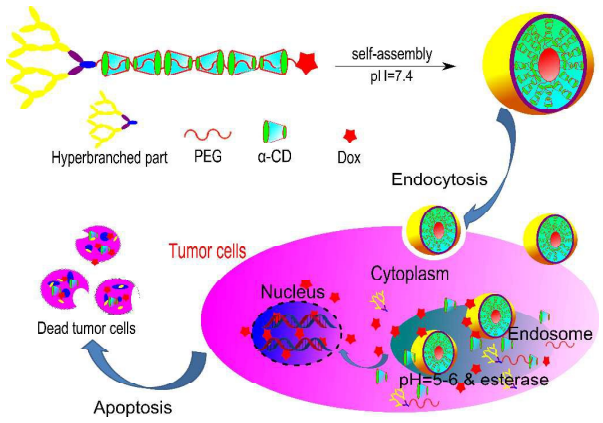

Scheme 1 Illustration on PR-g-DOX micelles selectively release drugs at endosomal compartments.

Experimental section

Materials

2,2-bis(hydroxymethyl)propionic acid (bis-MPA), 4-(dimethylamino) pyridine (DMAP), dicyclohexylcarbodiimide (DCC), N-hydroxysuccinimide (NHS), 2-(4-amidinophenyl)-6-indolecarbamidine dihydrochloride (DAPI), N，N，N′，N′，N″-pentamethyldiethylenetriamine (PMDETA) and methyl tetrazolium (MTT) were purchased from Aladdin Reagent Co., Ltd. (Shanghai, China). Poly(ethylene glycol) (PEG, Mn=2000), α-cyclodextrin was purchased from Sigma Aldrich (Shanghai, China). DOX was purchased from Beijing Huafeng United Technology Co.,Ltd (Beijing, China). Isopropylidene-2, 2-bis(methoxy)-propionic acid (bis-MPA), 4-(Dimethy1amino) pyridinium 4-Toluenesulfonate (DPTS) and compound **8** were prepared as previously reported.[40, 41] All other reagents were analytical grade and used directly without further purification. All solvents and water were redistilled freshly.

Instruments

The ^{1}H NMR spectra were recorded in deuterated dimethyl sulfoxide (DMSO-d_6) or deuterated chloroform ($CDCl_3$) using the 600 MHz spectrometer (Advance Bruker-600, Switzerland) with TMS as the internal reference. The crystalline changes of the products were confirmed by X-ray diffraction measurements, which were performed by using Cu-Ka irradiation with PHILP X'Pert MPD (20 kV; 35 mA; 2°/min). Fluorescence spectra were recorded on a Cary Eclipase fluorescence spectrophotometer. Surface tension was obtained using a contact angle meter (Dataphysics OCA40 Micro, Germany) with the pendant drop method at 25 °C. The zeta potential was measured by Zetasizer Nano ZS90 (Malvern, UK).The dynamic light scattering (DLS) was measured by BI-9000AT, BI-200SM, Brookhaven Instruments Co., USA. Transmission electron microscope (TEM) was measured by Jeol JEM-100CXat an accelerating voltage of 80 KV. Scanning electron microscopy (SEM) observation was performed on a Jeol JSM-5900LV electron microscope. The image of the DAPI dyed cells were recorded on a Nikon Eclipse Ti-E (Japan).

Synthesis of dendritic-polyrotaxane drug conjugate

The synthesis pathway of the dendritic-polyrotaxane drug conjugate is shown in Scheme S1 (in supporting information). The brief procedures for dendritic-polyrotaxane drug conjugate are described as follows:

mPEG 2000 (10.00 g, 5.00 mmol) was dissolved in 150 mL of CH_2Cl_2, followed by adding 3 mL of triethylamine and 4-toluene sulfonyl chloride (1.43 g, 7.50 mmol). The reaction solution was stirred for 24 h at room temperature and then extracted with 1 mol/L of HCl for three times. The organic phase was dried over anhydrous Na_2SO_4 and evaporated. The residue was dissolved in 10 mL of CH_2Cl_2, precipitated by addition of ether, harvested by filtration, and dried under vacuum to give product **1** as white crystals: 9.2 g (85.4%). ^{1}H NMR (600 MHz, $CDCl_3$): δ 2.45 (s, 3H, -ArCH_3), 3.58-3.64 (m, 185H, -OCH_2CH_2O-), 3.71 (t, J = 4.8 Hz, 2H, -CH_2CH_2OTs), 4.11 (t, J = 4.8 Hz, 2H, -CH_2CH_2OTs), 7.29 (d, J = 8.1 Hz, 2H, o-Ar), 7.74(d, J = 8.4 Hz, 2H, p-Ar).

Isopropylidene-2,2-bis(oxymethyl)-propionic acid (0.21 g, 1.15 mmol), compound **1** (2.02 g, 0.94 mmol), DCC (0.41 g, 1.99 mmol), DMAP (0.11 g, 0.91 mmol), and 50mL of CH_2Cl_2 were placed into a 100mL one neck round-bottom flask ice bath, and the reaction mixture was stirred for 48 h at room temperature. The dicyclohexylurea (DCU) was removed from the mixture by filtration, and the solvent was concentrated under reduced pressure, followed by liquid chromatography on Sephadex LH-20 gel with methanol as eluent to give the pure product **2** as white crystals: 2.06 g (94.9%). ^{1}H NMR (600 MHz, $CDCl_3$): δ 1.17 (s, 3H, -CH_3), 1.34 (s, 3H, -CH_3), 1.38 (s, 3H, -CH_3), 2.41 (s, 3H, -ArCH_3), 3.55 (d, J = 12Hz, 2H, -CH_2O), 3.58-3.64 (m, 185H, -OCH_2CH_2O-), 3.71 (t, J = 4.8 Hz, 2H, -CH_2CH_2OTs), 4.11 (t, J = 4.8 Hz, 2H, -CH_2CH_2OTs), 4.17 (d, J = 12Hz, 2H, -CH_2O), 4.28 (t, J = 4.8 Hz, 2H, -CH_2OOC-bis-MPA), 7.29 (d, J = 8.1 Hz, 2H, o-Ar), 7.74(d, J = 8.4 Hz, 2H, p-Ar).

Compound **2** (2.01 g, 0.87 mmol) was dissolved in 50 mL of methanol. Followed by one teaspoon of a Dowex, H^+ resin was added, and the reaction mixture was stirred for 5 h at room temperature. When the rection was complete, H^+ resin was filtered off in a glass filter and washed with methanol for twice. The methanol was evaporated to give product **3** as white crystals: 1.85 g (93.4%). ^{1}H NMR (600 MHz, $CDCl_3$): δ 1.19 (s, 3H, -CH_3), 2.41 (s, 3H, -ArCH_3), 3.56 (s, 4H, -CH_2OH), 3.58-3.64 (m, 185H, -OCH_2CH_2O-), 3.71 (t, J = 4.8 Hz, 2H, -

CH_2CH_2OTs), 4.11 (t, J = 4.8 Hz, 2H, -CH_2CH_2OTs), 4.28 (t, J = 4.8 Hz, 2H, -CH_2OOC-bis-MPA), 7.29 (d, J = 8.1 Hz, 2H, o-Ar), 7.74(d, J = 8.4 Hz, 2H, p-Ar).

Isopropylidene-2,2-bis(oxymethyl)- propionic acid (0.32 g, 1.75 mmol), compound **3** (1.51 g, 0.67 mmol), DCC (0.75 g, 3.64 mmol), DMAP (0.23 g, 1.89 mmol), and 50mL of CH_2Cl_2 were placed into a 100mL one neck round-bottom flask ice bath, and the reaction mixture was stirred for 72 h at room temperature. The dicyclohexylurea (DCU) was removed from the mixture by filtration, and the solvent was concentrated under reduced pressure, followed by liquid chromatography on Sephadex LH-20 gel with methanol as eluent to give the pure product **4** as white crystals: 1.42 g (82.6%). ^{1}H NMR (600 MHz, $CDCl_3$): δ 1.13 (s, 6H, -CH_3), 1.27 (s, 3H, -CH_3), 1.33 (s, 6H, -CH_3), 1.38 (s, 6H, -CH_3), 2.42 (s, 3H, -ArCH_3), 3.56 (d, J = 12Hz, 4H, -CH_2O), 3.58-3.64 (m, 185H, -OCH_2CH_2O-), 3.71 (t, J = 4.8 Hz, 2H, -CH_2CH_2OTs), 4.11 (t, J = 4.8 Hz, 2H, -CH_2CH_2OTs), 4.14 (d, J = 12Hz, 4H, -CH_2O), 4.29 (t, J = 4.8 Hz, 4H, -CH_2OOC-bis-MPA), 7.29 (d, J = 8.1 Hz, 2H, o-Ar), 7.74(d, J = 8.4 Hz, 2H, p-Ar).

Compound **4** (1.25 g, 0.48 mmol) was dissolved in 50 mL of methanol. Followed by one teaspoon of a Dowex, H^+ resin was added, and the reaction mixture was stirred for 12 h at room temperature. When the rection was complete, H^+ resin was filtered off in a glass filter and washed with methanol for twice. The methanol was evaporated to give as white crystals: 1.15 g (95.1%). ^{1}H NMR (600 MHz, $CDCl_3$): δ 1.09 (s, 6H, -CH_3), 1.28 (s, 3H, -CH_3), 2.41 (s, 3H, -ArCH_3), 3.56 (s, 8H, -CH_2OH), 3.58-3.64 (m, 185H, -OCH_2CH_2O-), 3.71 (t, J = 4.8 Hz, 2H, -CH_2CH_2OTs), 4.13 (t, J = 4.8 Hz, 2H, -CH_2CH_2OTs), 4.28 (t, J = 4.8 Hz, 4H, -CH_2OOC-bis-MPA), 4.36 (t, J = 4.8 Hz, 4H, -CH_2OOC-), 7.29 (d, J = 8.1 Hz, 2H, o-Ar), 7.74(d, J = 8.4 Hz, 2H, p-Ar). Then, isopropylidene-2,2-bis(oxymethyl)-propionic acid (0.58 g, 3.17 mmol), obtained white crystals (1.01 g, 0.41 mmol), DCC (1.35 g, 6.55 mmol), DPTS (0.51 g, 1.73 mmol), and 50mL of CH_2Cl_2 were placed into a 100mL one neck round-bottom flask under ice bath, and the reaction mixture was stirred for 96 h at room temperature. The dicyclohexylurea (DCU) was removed from the mixture by filtration, and the solvent was concentrated under reduced pressure, followed by liquid chromatography on Sephadex LH-20 gel with methanol as eluent to give the pure product as white crystals: 1.02 g (80.9%). ^{1}H NMR (600 MHz, $CDCl_3$): δ 1.12 (s, 12H, -CH_3), 1.25 (s, 9H, -CH_3), 1.33 (s, 12H, -CH_3), 1.39 (s, 12H, -CH_3), 2.43 (s, 3H, -ArCH_3), 3.56 (d, J = 12Hz, 8H, -CH_2O), 3.58-3.64 (m, 185H, -OCH_2CH_2O-), 3.71 (t, J = 4.8 Hz, 2H, -CH_2CH_2OTs), 4.11 (t, J = 4.8 Hz, 2H, -CH_2CH_2OTs), 4.14 (d, J = 12Hz, 8H, -CH_2O), 4.28 (m, 14H, -CH_2OOC-bis-MPA), 7.29 (d, J = 8.1 Hz, 2H, o-Ar), 7.74(d, J = 8.4 Hz, 2H, p-Ar). This obtained white crystal (0.95 g, 0.31 mmol) was then dissolved in 50 mL of methanol. Followed by one teaspoon of a Dowex, H^+ resin was added, and the reaction mixture was stirred for 24 h at room temperature. When the reaction was complete, H^+ resin was filtered off in a glass filter and washed with methanol for twice. The methanol was evaporated to give product **5** as white crystals: 0.85 g (94.4%). ^{1}H NMR (600 MHz, DMSO-d_6): δ 1.06 (s, 12H, -CH_3), 1.10 (s, 6H, -CH_3), 1.19 (s, 3H, -CH_3), 2.41 (s, 3H, -ArCH_3), 3.55 (s, 16H, -CH_2OH), 3.58-3.64 (m, 185H, -OCH_2CH_2O-), 3.71 (t, J = 4.8 Hz, 2H, -CH_2CH_2OTs), 4.11-4.28 (m, 16H, -CH_2OOC-bis-MPA & -CH_2CH_2OTs), 7.29 (d, J = 8.1 Hz, 2H, o-Ar), 7.74(d, J = 8.4 Hz, 2H, p-Ar).

Sodium azide (0.10 g, 1.54 mmol) was added to the solution of compound **5** (0.51 g, 0.17 mmol) in 25 mL DMF under nitrogen and the mixture was placed in an oil bath maintained at 30 °C for 24 h. The resulting solution was cooled to ambient temperature and filtered to remove the sodium azide. After removing DMF under reduced pressure, the residue was dissolved in methanol and followed by liquid chromatography on Sephadex LH-20 gel with methanol as eluent to give the pure product **6** as yellow crystals: 0.43 g (87.8%). ^{1}H NMR (600 MHz, $CDCl_3$): δ 1.06 (s, 12H, -CH_3), 1.10 (s, 6H, -CH_3), 1.19 (s, 3H, -CH_3), 3.36 (t, 2H, -CH_2N_3), 3.55 (s, 16H, -CH_2OH), 3.58-3.64 (m, 185H, -OCH_2CH_2O-), 4.11-4.28 (m, 14H, -CH_2OOC-bis-MPA).

An aqueous solution (100 mL) of product **6** (1.00 g, 0.028 mmol) and α-CD (12.00 g, 12.94 mmol) was ultrasonically agitated at room temperature for 5 min and then stirred overnight at ambient temperature to form pseudo-PR, the precipitate was collected by centrifugation, washed with 30 mL deionized water for more than 5 times and then dried under vacuum at 65 °C for 24 h, affording pseudo-PR **7** as white powder. Yield: 55.6 mg. ^{1}H NMR (600 MHz, DMSO-d_6): δ 1.06 (s, -CH_3), 1.10 (s, -CH_3), 1.19 (s, -CH_3), 3.25-3.40 (br overlapped, H-2,4 & -CH_2N_3), 3.50-3.79 (br overlapped, H-3,5,6 & -CH_2OH), 4.11-4.28 (m, -CH_2OOC-bis-MPA), 4.75 (m, H-1), 5.35-5.55 (m, OH-2,3).

Pseudo-PR **7** (100.1 mg) was dissolved in 5 mL of dry DMF under N_2. Then, CuBr (5.3 mg), PMDETA (10.1 μL), compound **8** (30.2 mg) were added successively. After stirring for 24h in darkness at ambient temperature, the reaction system was transferred into a dialysis bag (MWCO 3500) and dialyzed against 5 L deionized water for 2 days to remove PMDETA, catalyst, and excessive compound **8**. Then the liquid in the dialysis bag was lyophilized to afford the dendritic-polyrotaxane drug conjugate **9** as red powder. Yield: 55.6 mg. ^{1}H NMR (600 MHz, DMSO-d_6): δ 1.06 (s, -CH_3), 1.10 (s, -CH_3), 1.19 (s, -CH_3), 3.25-3.40 (br overlapped, H-2,4 & -CH_2N_3), 3.50-3.79 (br overlapped, H-3,5,6 & -CH_2OH), 4.11-4.28 (m, -CH_2OOC-bis-MPA), 4.75 (m, H-1), 5.35-5.55 (m, OH-2,3), 6.55–8.50 (m, H of benzene rings on DOX). The content of DOX conjugated to the pseudo-PR was determined by using fluorescence with a slit width of 5.0 and 5.0 nm for excitation and emission. The emission wavelength was 485 nm and the excitation wavelength was 560 nm, giving 1.84% (wt %) of drug loading content.

Preparation and characterization of the dendritic-polyrotaxane drug conjugate micelles solution

The dendritic-polyrotaxane drug conjugate **9** (10 mg) was dissolved in 4 mL of deionized water and stirred for 24 h in dark. The obtained solution was kept at 4°C in refrigerator under Ar protection for future use.

The critical micelle concentration (CMC) of dendritic-polyrotaxane drug conjugate micelles was determined by the surface tension methods.[1] The concentration of dendritic-polyrotaxane drug conjugate **9** micelles was varied from 0.001 to 1 mg/ml and data were obtained using a contact angle meter with the pendant drop method at 25 °C.

The size of the dendritic-polyrotaxane drug conjugate **9** in aqueous solutions (1 mg/ml) were measured by dynamic light scattering (DLS) at 25 °C using a Coherent innove 304 laser electronic source at the wavelength 532 nm; the scattering angle is 90 ◦. Each sample was measured three times, and the results shown are the mean diameter for two replicate samples.

Samples solution (1 mg/ml) were dropped onto copper grid and dried at room temperature. The samples were stained

with phosphotungstic acid (ATP) aqueous solution and dried in air. TEM observations were performed at an accelerating voltage of 80 kV and 300 kV. The samples (micelle concentration of 10 mg/mL) were prepared by directly dropping the solution of micelles onto slice of silicon and dried at room temperature overnight for SEM studies.

The zeta potential of the micelles was characterized using a Zetasizer Nano ZS90 (Malvern, UK). The dendritic-polyrotaxane drug conjugate was diluted to 10 mL with PBS to a final concentration of 1 mg/mL.

The pH-triggered hydrolysis rate of the dendritic-polyrotaxane drug conjugates

The hydrolysis of dendritic-polyrotaxane drug conjugate **9** with hydrazone bond at different pH values (5.0, 6.0 and 7.4) was performed as follows: first, dendritic-polyrotaxane drug conjugate **9** (1 mg) was dissolved in 2 mL phosphate buffered saline solution (PBS) with different pH values (pH 5.0, 6.0 and pH 7.4) and were placed in dialysis bags (MWCO, 3500 Da) and dialyzed against 10 ml of PBS at 37 °C with constant shaking. Then, 4 ml medium was removed and replaced by 4 mL fresh PBS to maintain submersed conditions at desired time intervals. The released amount of the DOX was determined using fluorescence with a slit width of 5.0 and 5.0 nm for excitation and emission. The emission wavelength was 485 nm and the excitation wavelength was 560 nm. The release experiments were carried out in triplicate. The results presented are the average data.

Cell viability assays

The biocompatibility of the prodrug was evaluated using the methyl tetrazolium (MTT) assay in a 96-well plate method. A549 and HepG2 cells were cultured in 96 well culture plates at a density of 6000 cells per well in RPMI 1640 medium supplemented with 10 % fetal bovine serum at 37 °C in humidified environment of 5 % CO_2 for 1 day. The cells were then incubated with PR-g-DOX, pseudo-PR, DOX and compound **8** at varing concentrations of 0.25-6 μg DOX-equivalent dose by RPMI 1640 medium containing 10 % fetal bovine serum and incubated for another 72 h at 37 °C in humidified environment of 5 % CO_2 . Then, the RPMI 1640 medium was aspirated and replaced with 100 μl fresh RPMI 1640 medium containing 10 % fetal bovine serum for 24h. Then 10 μl 5 mg/ml MTT solution was added to each well and incubated for another 4 h at 37 °C in humidified environment of 5 % CO_2. The medium solution was then replaced with 150 μl DMSO to dissolve the MTT-formazan that generated by live cells and the plate were shaked for 30 min to produce a homogeneous colored solution. The absorbance was then read at wavelength 570 nm on a microplate reader. The relative cell viability (%) was determined by comparing the absorbance at wavelength 570 nm with control cells containing only cell culture medium at wavelength 570 nm. The experiments were carried out six times and results presented are the average data.

Cellular uptake and localization of micelles

About 20000 A549 cells in 2 mL of RPMI-1640 medium containing 10 % fetal bovine serum were seeded per well in a 6-well culture plates that contained a sterile glass coverslip in each well. Then the plate was incubated for 24 h at 37 °C in a humidified environment of 5 % CO2 and 95 % air. The original medium was then removed and replaced with 2 mL of fresh medium and dropped into 100 μl of dendritic-polyrotaxane drug conjugate **9** (100 μg/mL). At the appropriate time point, the RPMI 1640 medium was aspirated and the cells were rinsed three times with PBS. Then 0.5 mL of 4 % paraformaldehyde was dropped into each well to fix the cells for 15 min. Then the paraformaldehyde was aspirated, the cells after being rinsed three times with PBS were stained with 0.5 mL 1μg/mL DAPI solution for 15 min. Then DAPI staining solution was removed and the cells were washed by PBS twice before coverslips were mounted on the slides by a drop of permount.[42] Images were taken using a Nikon Eclipse Ti-E microscope. DOX was observed using a Cy3 filter expressed as red and DAPI was observed using a DAPI filter expressed as blue..

In vivo anticancer activities

The experiment was carried out using male Chinese Kun Ming mice (body weight about 25-30 g) and the mice were handled under protocols approved by Sichan University Laboratory Animal Center. 24 mice were divided into four groups with equal amount and maintained under sterile conditions and 12 h light/dark cycle in a temperature-controlled environment. The mice were implanted with S180 tumor cells in subaxillary, and 1 week after implantation, the tumors along the subaxillary were well established. The mice were randomly divided into four groups (n = 6). Then four groups of mice were administered 4 times at day 1, 4, 7, 10 with 4 mg/kg doxorubicin equivalents of DOX, Pseudo-PR, dendritic-polyrotaxane drug conjugate **9** and physiological saline (used as control reagent) via the tail vein in a final volume of 200 μL respectively. The body weights of mice were measured, whereas the behaviors of animals were detected by the animal health care technicians every day. After 10 days dosing period, surviving mice were allowed to recover and weight was monitored continuously 10 days. Then the mice were sacrificed and all the tumors in the bodies were dissected for the tumor weight.

Maximum tolerated dose studies

Kunming mice were divided into 8 groups (n = 6) and administered intravenously with the free DOX or PR-g-DOX (5, 10, 15, 20 mg/kg doxorubicin equivalents body weight in 200 μL saline) for a single injection and then allowed to recover and weight was monitored continuously 9 days. Changes in body weight and survival of mice were measured daily for the whole 10 days. The maximum tolerated dose (MTD) was defined as the maximum plitidepsin dose resulting in less than 15% loss in body weight and that does not cause death.[43]

Results and discussion

Synthesis and characterization of PR-g-DOX

It has been reported that PRs with end-capping group as a kind of drug delivery system.[27] For instance, through the hydroxy groups on the PR and a hydrophilic spacer, Yu et al. reported a succinate-based PTX ester derivative was attached to the PR covalently and the PTX release can be accelerated by esterase catalysis. However, ester bond was not sensitive enough to the mildly acidic pH in tumor tissues and at endosomal compartments.[44] As far as we known, pH-sensitive dendritic-polyrotaxane drug conjugates have not been reported. In this paper, the hydrazone bond was chosen as the pH responsible linking bond for preparation of dendritic-

polyrotaxane drug conjugates because it is easy to be hydrolyzed in mildly acidic environment. Amphiphilic polymer molecular composed of hydrophilic and hydrophobic segments could be assembled into a core-shell structure in certain solvent. We proposed that dendritic-polyrotaxane drug conjugates would be similar to a surfactant-like amphiphilic molecule that self-assemble to micellar nanoparticles in water, leading to a fixed DOX-loading content. Therefore, the hyperbranched part with eight hydroxyl groups of the conjugate as the hydrophilic part of the conjugates while the inclusion part that formed between cyclodetrin and PEG as the hydrophobic part of the conjugate.

The DOX with a terminal alkynyl group (compound **8**) was firstly synthesized according the previous paper, and the compound **6** with a hyperbranched group at one end and an azido group at another end was synthesized through a series of precise reactions. Then the Pseudo-PR **7** was obtained by complexation of α-cyclodextrin with PEG chain in water. Figure 1 shows the X-ray diffraction (XRD) patterns of the PEG/α-CD inclusion complex, Pseudo-PR, α-CD, PR-g-DOX and compound **6**. It can be seen that the patterns of PR-g-DOX and Pseudo-PR are different from that of compound **6** or α-CD. The peaks for the PR-g-DOX and Pseudo-PR at 2θ = 19.9º are consistent with the peak for the PEG/α-CD inclusion complex at 2θ = 19.9º, indicating the formation of the PEG/α-CD inclusion structures in PR-g-DOX and Pseudo-PR.[41] However, it's not simple to the conjugating of compound 6 to the Pseudo-PR **7**, since the high molecular weight of the two compounds lead to relatively larger stereospecific blockade. In an alternative way, the pseudo-PR **7** with azido group at one end was covalently linked to the compound **6** via CuI-catalyzed azide alkyne cycloaddition (CuAAC), resulting in the final dendritic-polyrotaxane drug conjugate. The reaction could be completed via the high efficiency of click chemistry.[45] Therein, ^{1}H NMR spectra of dendritic-polyrotaxane drug conjugate **9** showed the presence of triazole proton of 7.81 ppm which indicated the formation of the 1,4-regioisomer exclusively. The fluorescence of the dendritic-polyrotaxane drug conjugate attributed to the inherent fluorescence of DOX, and the result proved the DOX was conjugated to the pseudo-PR **7** successively.

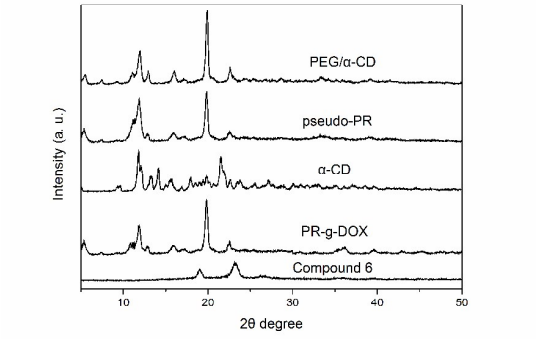

Figure 1 X-ray diffraction patterns of PEG/α-CD, pseudo-PR, α-CD, PR-g-DOX and compound 6.

Size, morphology and zeta potential of the dendritic-polyrotaxane drug conjugate micelles

The CMC for the dendritic-polyrotaxane drug conjugate **9** micelles was determined by the surface tension method. Usually, the amphiphilic copolymer concentration is above CMC and these polymeric micelles are formed to minimize the interfacial energy, while the interfacial tension shows a sudden change at or near CMC, so the surface tension measurements should be carried out over a wide range of concentrations. Figure S3 shows that the surface intension decreases linearly with the logarithmic copolymer concentrations at low concentrations but is flat in the crossover region. So the CMC of dendritic-polyrotaxane drug conjugate **9** formed micelles determined from the intersection point of those two straight lines is about 0.016 mg/ml.

As dynamic light scattering (DLS) results shown, the mean diameter of the drug conjugate **9** micelles in water (pH=7.4) were about 120 nm with narrow size distributions (PDI = 0.106) (Figure 2a). Normally, the segments that producing drive force are needed to introduce to the PEGylation and functionlization of dendron for the self-assembly. So, for our designed molecular, self-assembly behavior should be mediated by dendritic-polyrotaxane drug conjugate itself. We assumed two major driving force in our system, the primary driving force responsible for the self-assembly behavior is the minimization of the interfacial energy governed by the balance between the hydrophilic interaction of the branched hydroxy groups and the hydrophobic interaction of the polyrotaxane blocks. Secondly, the driving forces governed self-assembly of the drug conjugate should be come from the linked DOX, such as π-π stacking, dipole interactions and H-bonding, since the DOX is composed of multiple domains of different chemical composition, e.g., hydrophobic, aliphatic and aromatic. The zeta potential value of drug conjugate micelles was measured, showing a slightly positive charge about 2.5 mV (Figure 2b), which may be due to the ionization of the amino group on DOX.

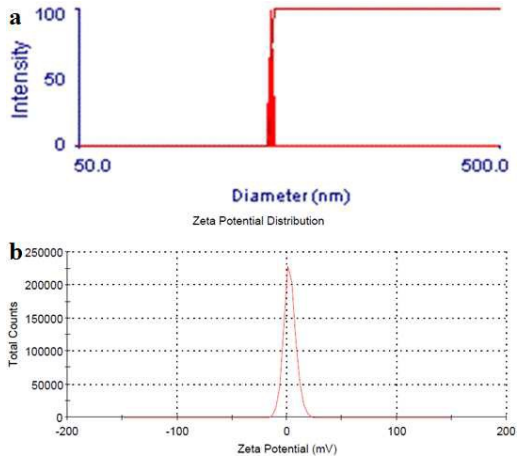

Figure 2 The DLS (a) and zeta potential (b) results of dendritic-polyrotaxane drug conjugate **9** based micelles.

Furthermore, TEM and SEM results were also performed to demonstrate the formation of micellar nanoparticles from dendritic-polyrotaxane drug conjugate **9**, resulting in uniform spherical shapes with diameters around 110 nm (Figure 3). However, the size of the micelles observed in TEM and SEM were slightly smaller than detected by DLS, the difference should be due to the shrinkage of particles during the process of the solvent evaporation in the sample preparation for both of TEM and SEM. As shown SEM and TEM, the compact

nanoparticle may be due to the strong aggregation of dendritic-polyrotaxane drug conjugates via non-covalent forces mediated by polyrotaxane blocks and DOX. Thus, the micellar nanoparticle has a core/shell structure composed of a hydrophobic inner core containing polyrotaxane blocks and DOX molecules and a branched hydroxy group shell layer. These proper defined micelles may have the potential lead to high antitumor efficacy via EPR effect.[8, 46]

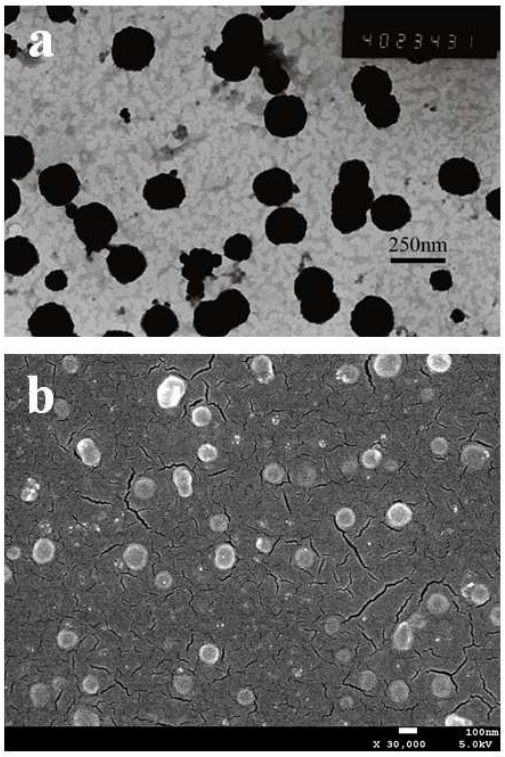

Figure 3 a) TEM and b) SEM results of dendritic-polyrotaxane drug conjugate **9** based micelles. The scale bars correspond to 250 nm for TEM and 100 nm for SEM.

Stimuli responsive release behavior of micelles

The DOX releasing behaviors from dendritic-polyrotaxane drug conjugate **9** micelles was investigated under three different pHs (5.0, 6.0 and 7.4) at 37 °C. The cumulative release amount of the DOX was determined by fluorescence spectroscopy method. Interestingly, the results showed that approximately 85 and 73% of DOX were released in 300 h, at pH 5.0 and 6.0, respectively, from drug conjugate micelles. In contrast, only 25% of DOX was released after 300 h at pH 7.4 (Figure 4). These results indicate that drug conjugates are acid-sensitive and more likely cleavable at acidic endosoma or tumor, while stable at physiological environment. Moreover, almost no burst release in aqueous solution was observed at pH 7.4 in prior 24 h (Figure S11 in supporting information), so this acid-sensitive drug conjugate would be more stable than most of other drug delivery systems in the blood compartments and has obvious advantages over other reported acid-sensitive conjugates, that is, enhanced pH-sensitivity and potential for superior site-specific delivery.

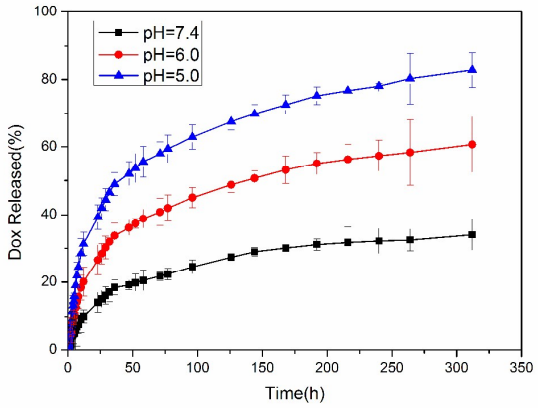

Figure 4 pH-Triggered hydrolysis of DOX in the dendritic-polyrotaxane drug conjugate **9** micelles (n=3).

Intracellular uptake of the PR-g-DOX micelles

A549 lung cancer cell lines were used for the examination of intracellular uptake of the dendritic-polyrotaxane drug conjugate PR-g-DOX, the nuclei of the tumor cells were stained with DAPI. As shown in Figure 5, significant DOX fluorescence was observed at the perinuclear as well as nuclei of A549 cells after 1h of incubation with PR-g-DOX (Figure 5b-c). Following 4 h of incubation, more DOX was accumulated at the nuclei of A549 lung cancer cells (Figure 5e-f), suggested that more and more micelles were internalized. After 8 h of incubation, DOX was predominantly accumulated at the nuclei of A549 cells (Figure 5h-i). DOX, one of the most potent anticancer drugs used widely in the treatment of different types of solid malignant tumors, is known to exert drug effects via intercalation with DNA and inhibition of macromolecular biosynthesis.[47] It is of particular interest, therefore, that dendritic-polyrotaxane drug conjugate **9** micelles are able to deliver and release DOX right into the cell nucleus.

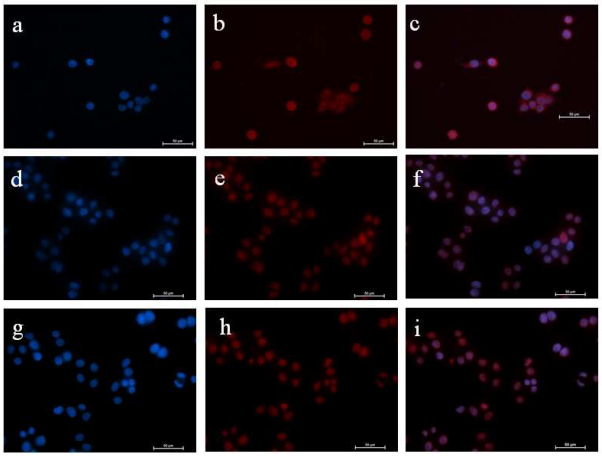

Figure 5 The fluorescent images of A549 lung cancer cells incubated with PR-g-DOX for (a-c) 1, (d-f) 4, and (g-i) 8 h. For each panel, images from left to right show cell nuclei stained by DAPI (blue), DOX fluorescence in cells (red), , and overlays of two images. The scale bars correspond to 50 μm in all images.

In vitro anticancer activities

The responsive micelles are good candidates for drug delivery system. The cytotoxicities of PR-g-DOX, pseudo-PR, compound **8** and DOX were investigated in A549 cancer cell lines by MTT assays. As shown in Figure 6a, the activity of PR-g-DOX was much higher than that of DOX at lower concentrations from 0.1-0.5 μg/mL. For example, significantly reduced cell viabilities of about 48.6, 64.9, 78.8 % were observed for PR-g-DOX at concentration of 0.1, 0.25, 0.5 μg/mL (doxorubicin-equivalent concentrations) for A549 respectively, while free DOX only reduced cell viabilities of about 40.3, 54.3 and 69.9% at the same concentrations. The half maximal inhibitory concentration (IC_{50}) of PR-g-DOX was 0.11 μg/mL for A549 cancer cells, while IC_{50} of DOX was 0.20 μg/mL, which was about 2-folder of that for PR-g-DOX. Therefore, the PR-g-DOX clearly enhanced cytotoxicity of DOX. Meanwhile, the PR-g-DOX was found to be highly cytotoxicity at low concentrations to A549 cancer cell lines in comparison with compound **8** (doxorubicin-equivalent concentrations). The result showed in Figure 6b revealed that pseudo-PR used for synthesizing PR-g-DOX was almost nontoxic to the cells when the tested concentration was up to 180 μg/mL, which indicating that pseudo-PR inherited excellent biocompatibility property of PEG and α-cyclodextrin. In conjunction with the above results, we can conclude that PR-g-DOX could be served as a prodrug that has the ability to releases active DOX once inside cancer cells inducing their apoptosis. So all the results obtained above indicate the PR-g-DOX would be a good candidate for cancer treatment.

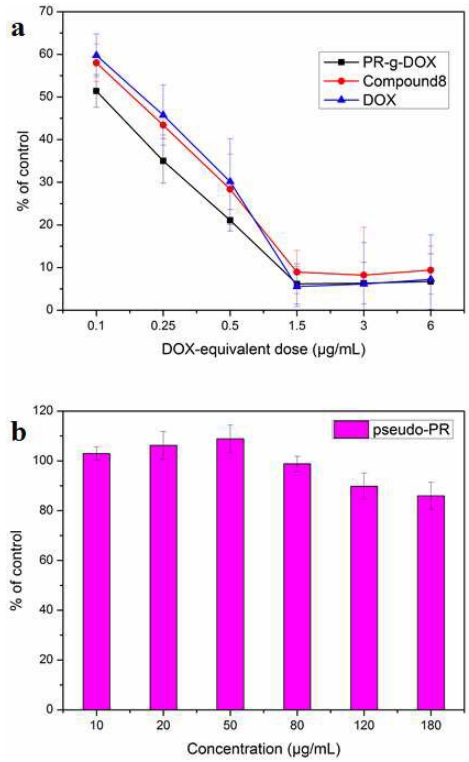

Figure 6 The in vitro efficacy. a) In vitro cytotoxicity of PR-g-DOX, Compound **8** and free DOX to A549 lung cancer cells; b) the cytotoxicity of pseudo-PR. Values represent average ± s.d. (n=6)..

In vivo anticancer activities

The therapeutic efficacy of PR-g-DOX micelles and pseudo-PR compared to free DOX were evaluated using KM mice bearing S180 sarcoma tumors in subaxillary, while the saline was used as control. It should be noted that PR-g-DOX, pseudo-PR and DOX were dissolved in saline solution for i.v. administration due to the inherent water solubility with the concentration of 4 mg/kg equivalents of DOX in 200 μL saline for every injection, and the agents were applied every three days for 10 days, then the mice were allowed to recover for another 10 days, at the end of this in vivo experiment, the tumors of all different groups were removed and weighted. As shown in Figure 7a, compared the treatment group with the control group, PR-g-DOX showed almost 2-fold tumor growth inhibition in tumor model ($p < 0.001$), and free DOX only showed moderate antitumor efficacy compared to the PR-g-DOX group ($p < 0.05$). The significance of the experimental data was determined by a Student's t-test and data are plotted as means ± standard errors (SE). The high antitumor activity of the micelles may be due to the potential higher accumulation in tumor via EPR effect and the accelerated release of DOX from endosomes. The results demonstrated the high therapeutic potential of the PR-g-DOX micelles. Moreover, monitoring of the body weight of the tumor burdened animals was carried out during the whole period of the experiments, the results showed that only less body weight shift was observed for the group administrated micelles and no significant weight loss for the group administrated pseudo-PR while the DOX treated ones almost lost 20% of their initial weight (Figure 7b). Furthermore, the clinical signs, body weight changes on normal mice were also carried out to evaluate the safety of the PR-g-DOX micelles used as drug delivery. So, these parameters for assessing in vivo toxicity of PR-g-DOX micellar nanoparticles, pseudo-PR and DOX were recorded in the experiment and the physiologic saline as control. The experiment process was as same as the above in vivo anticancer activities experiment except the tumor burdened mice were changed as normal mice. As recorded and shown in Figure 7c, during the whole period, no adverse effects on their growth were observed for the mice administrated saline as evident in their normal body weight increased steadily, the group injected PR-g-DOX micelles exhibited slight body decrease compared to the saline group and the group injected pseudo-PR exhibited slight body increase compared to the saline group, and these two body shift results were close to that of the control group, showing the good biocompatibility of PR-g-DOX micelles. However, the obvious body shifted for DOX administrated mice, resulting in about 20% weight lost. Moreover, throughout the study period of 20 days, the mice administrated PR-g-DOX micelles, pseudo-PR and saline showed no apparent signs of dehydration, locomotor impairment, muscle loss, anorexia and other symptoms associated with animal toxicity. All these results indicated the better drug tolerability of the PR-g-DOX micelles and a higher in vivo efficacy without increasing its toxicity of the PR-g-DOX micellar nanoparticles.

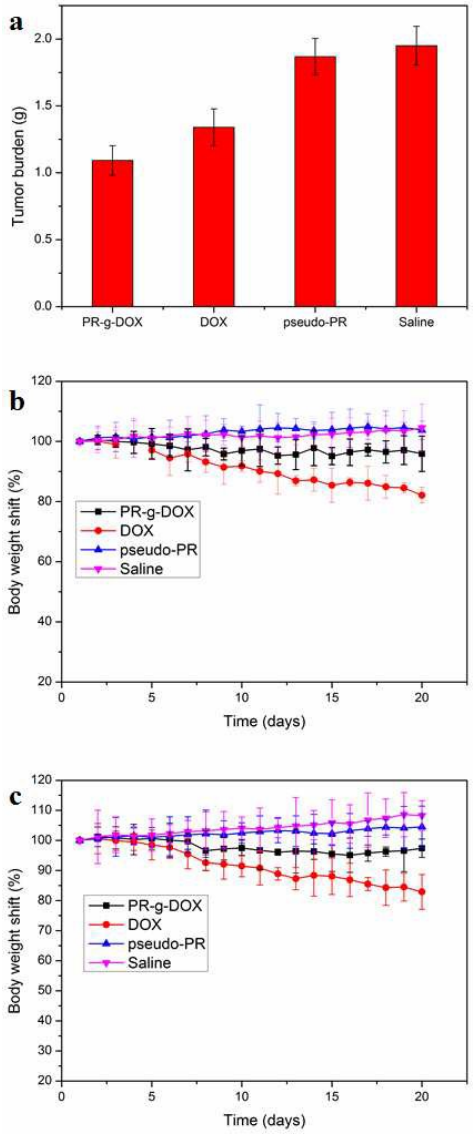

Figure 7 The in vivo efficacy. a) In vitro antitumor activity of PR-g-DOX, pseudo-PR and free DOX to allografted S180 sarcoma tumors in KM mice; b) the body weight shift of the tumor burdened KM mice of PR-g-DOX, pseudo-PR and free DOX; c) the body weight shift of the normal KM mice of PR-g-DOX, pseudo-PR and free DOX. Values represent average ± s.d. (n=6).

Maximum tolerated dose studies

The MTD for a single dose of PR-g-DOX micelles was assessed in tumor free Kunming mice and compared with free DOX by administered intravenously with different doses of PR-g-DOX micelles or free DOX, followed by daily body weight measurement and observation of toxic death for another 9 days. As shown in Figure 8, the MTD result for the free DOX was about 5 mg/kg. By increasing free DOX dosage to 10 mg/kg, 50% of the treated mice died in 8 days, the result was closed to the report that LD_{50} of DOX (the lethal dose for killing 50% of the test animals within a designated period) is 12 mg/kg. In contrast, there was only 3% body weight loss and no toxic death for the mice treated with PR-g-DOX micelles at a DOX equivalent dosage as high as 10 mg/kg, even treated with PR-g-DOX micelles at a DOX equivalent dosage as high as 15 mg/kg, only about 3% body weight loss and only about one death occurred. From the present study, it can be estimated that the single i.v. MTD for PR-g-DOX micelles was at least 10mg/kg, which was 2-fold of that for free DOX. The high MTD for PR-g-DOX micelles may be attributed to the slow release kinetics of DOX without burst release under physiological conditions and the remarkable biocompatibility and safety of the pseudo-PR, which was mainly constituted by α-cyclodextrin and PEG.

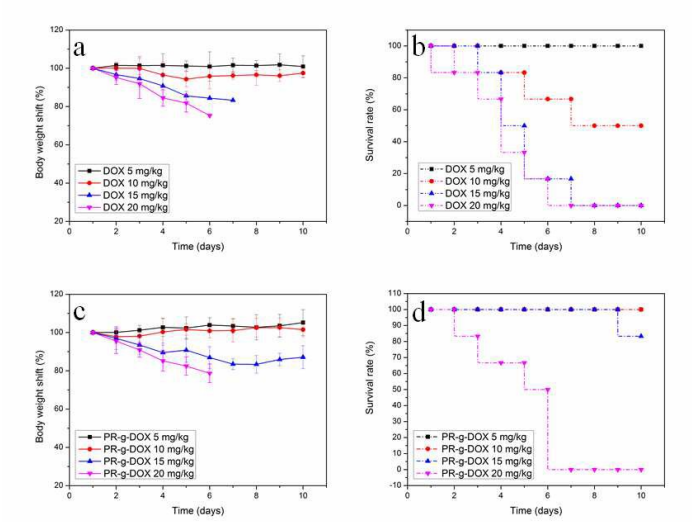

Figure 8 MTD studies for free DOX (a, b) and PR-g-DOX micelles (c, d) on body weight change and survival rate in tumor-free Kunming mice.

Conclusions

We have designed and successfully fabricated a kind of pH-sensitive liner-dendritic drug-polymer conjugate by conjugating DOX to the end of dendritic polyrotaxane via hydrazone bond. This drug-polymer conjugate could form stable micelles (PR-g-DOX micelles) in water with diameters around 110 nm observed in TEM and SEM. These PR-g-DOX micelles showed a significantly faster DOX release at mildly acidic pH of 6.0 and 5.0 while without burst release in aqueous at a physiological pH of 7.4. The intracellular uptake assay and in vitro anticancer activities confirmed that the PR-g-DOX micelles could efficiently delivery DOX to the nuclear of the tumor cells, and led to much more cytotoxic effects to A549 over parent DOX. In vivo, the PR-g-DOX micelles showed significantly tumor inhibition and the MTD results showed PR-g-DOX micelles had an excellent safety profile, with MTD of 10 mg/kg equivalent dose of DOX , which was a folder higher than that (5 mg/kg DOX) for free DOX. It is believed that this kind of micelle will have potentials as intelligent nanocarrier for passive targeted cancer therapy.

Acknowledgements

This work was funded by the National Natural Science Foundation of China (Grant Nos. 51373174), the CAS Knowledge Innovation Program (Grant No. KSCX2-EW-J-22) and West Light Foundation of CAS.

Notes and references

[a] Key Laboratory of Mountain Ecological Restoration and Bioresource Utilization, Chengdu Institute of Biology, Chinese Academy of Sciences,

Chengdu 610041, China, Tel: +86-28-82890646. Fax: (+86)28-82890646. E-mail: libj@cib.ac.cn (B. Li)

[b] State Key Laboratory of Polymer Materials Engineering, Polymer Research Institute of Sichuan University, Sichuan University, Chengdu 610065, China, Tel, Fax: +86-28-85400266. E-mail: zslbj@163.com (S. Zhang).

Electronic Supplementary Information (ESI) available: The synthesis pathway of the dendritic-polyrotaxane drug conjugate. ^{1}H NMR spectra of compounds **1**-**9**. Releasing behaviors of DOX in prior 25 h. Standard curve plotted by the excitation wavelength was 560 nm excited by 485 nm versus the DOX concentration. See DOI: 10.1039/b000000x/

1. Y. Kang, W. Ha, Y.-Q. Liu, Y. Ma, M.-M. Fan, L.-S. Ding, S. Zhang and B.-J. Li, *Nanotechnology*, 2014, **25**, 335101.
2. K. Wang, Y. Liu, C. Li, S.-X. Cheng, R.-X. Zhuo and X.-Z. Zhang, *ACS Macro Letters*, 2013, **2**, 201-205.
3. Y. Kang, K. Guo, B.-J. Li and S. Zhang, *Chemical Communications*, 2014, **50**, 11083-11092.
4. E. Serrano, G. Rus and J. Garcia-Martinez, *Renewable and Sustainable Energy Reviews*, 2009, **13**, 2373-2384.
5. J.-F. Gohy and Y. Zhao, *Chemical Society Reviews*, 2013, **42**, 7117-7129.
6. J. Huang and A. Heise, *Chemical Society Reviews*, 2013, **42**, 7373-7390.
7. F. Meng, Z. Zhong and J. Feijen, *Biomacromolecules*, 2009, **10**, 197-209.
8. A. Jhaveri, P. Deshpande and V. Torchilin, *Journal of Controlled Release*, 2014.
9. X. Ma, Y. Zhao and X.-J. Liang, *Accounts of chemical research*, 2011, **44**, 1114-1122.
10. H. Wei, S.-X. Cheng, X.-Z. Zhang and R.-X. Zhuo, *Progress in Polymer Science*, 2009, **34**, 893-910.
11. C.-L. Liu, C.-H. Lin, C.-C. Kuo, S.-T. Lin and W.-C. Chen, *Progress in Polymer Science*, 2011, **36**, 603-637.
12. M. S. Shim and Y. J. Kwon, *Advanced drug delivery reviews*, 2012, **64**, 1046-1059.
13. E. Fleige, M. A. Quadir and R. Haag, *Advanced drug delivery reviews*, 2012, **64**, 866-884.
14. X.-B. Xiong, A. Falamarzian, S. M. Garg and A. Lavasanifar, *Journal of Controlled Release*, 2011, **155**, 248-261.
15. M. Motornov, Y. Roiter, I. Tokarev and S. Minko, *Progress in Polymer Science*, 2010, **35**, 174-211.
16. J. Zhuang, M. R. Gordon, J. Ventura, L. Li and S. Thayumanavan, *Chemical Society Reviews*, 2013, **42**, 7421-7435.
17. R. Cheng, F. Meng, C. Deng, H.-A. Klok and Z. Zhong, *Biomaterials*, 2013, **34**, 3647-3657.
18. I. Gitsov, K. R. Lambrych, V. A. Remnant and R. Pracitto, *Journal of Polymer Science Part A: Polymer Chemistry*, 2000, **38**, 2711-2727.
19. E. Blasco, M. Piñol and L. Oriol, *Macromolecular Rapid Communications*, 2014.
20. I. Javakhishvili, W. H. Binder, S. Tanner and S. Hvilsted, *Polymer Chemistry*, 2010, **1**, 506-513.
21. E. R. Gillies and J. M. Frechet, *Drug Discovery Today*, 2005, **10**, 35-43.
22. R. S. Dhanikula and P. Hildgen, *Biomaterials*, 2007, **28**, 3140-3152.
23. K. Luo, C. Li, L. Li, W. She, G. Wang and Z. Gu, *Biomaterials*, 2012, **33**, 4917-4927.
24. R. Duncan and L. Izzo, *Advanced Drug Delivery Reviews*, 2005, **57**, 2215-2237.
25. N. Malik, R. Wiwattanapatapee, R. Klopsch, K. Lorenz, H. Frey, J. Weener, E. Meijer, W. Paulus and R. Duncan, *Journal of Controlled Release*, 2000, **65**, 133-148.
26. Y. He, P. Fu, X. Shen and H. Gao, *Micron*, 2008, **39**, 495-516.
27. F. van de Manakker, T. Vermonden, C. F. van Nostrum and W. E. Hennink, *Biomacromolecules*, 2009, **10**, 3157-3175.
28. M. Messner, S. V. Kurkov, P. Jansook and T. Loftsson, *International Journal of Pharmaceutics*, 2010, **387**, 199-208.
29. A. Harada and M. Kamachi, *Macromolecules*, 1990, **23**, 2821-2823.
30. G. Yu, M. Xue, Z. Zhang, J. Li, C. Han and F. Huang, *Journal of the American Chemical Society*, 2012, **134**, 13248-13251.
31. G. Yu, X. Zhou, Z. Zhang, C. Han, Z. Mao, C. Gao and F. Huang, *Journal of the American Chemical Society*, 2012, **134**, 19489-19497.
32. G. Yu, Y. Ma, C. Han, Y. Yao, G. Tang, Z. Mao, C. Gao and F. Huang, *Journal of the American Chemical Society*, 2013, **135**, 10310-10313.
33. J. Li, X. Li, X. Ni, X. Wang, H. Li and K. W. Leong, *Biomaterials*, 2006, **27**, 4132-4140.
34. X. Ni, A. Cheng and J. Li, *Journal of Biomedical Materials Research Part A*, 2009, **88**, 1031-1036.
35. J. Liu, H. R. Sondjaja and K. C. Tam, *Langmuir*, 2007, **23**, 5106-5109.
36. N. Yui, R. Katoono and A. Yamashita, in *Inclusion Polymers*, Springer, 2009, pp. 115-173.
37. C. Yang, X. Wang, H. Li, J. Ling Ding, D. Yun Wang and J. Li, *Polymer*, 2009, **50**, 1378-1388.
38. T. Ooya, H. S. Choi, A. Yamashita, N. Yui, Y. Sugaya, A. Kano, A. Maruyama, H. Akita, R. Ito and K. Kogure, *Journal of the American Chemical Society*, 2006, **128**, 3852-3853.
39. M. M. Fan, X. Zhang, J. Qin, B. J. Li, X. Sun and S. Zhang, *Macromolecular Rapid Communications*, 2011, **32**, 1533-1538.
40. J. S. Moore and S. I. Stupp, *Macromolecules*, 1990, **23**, 65-70.
41. K.-L. Dao, R. R. Sawant, J. A. Hendricks, V. Ronga, V. P. Torchilin and R. N. Hanson, *Bioconjugate Chemistry*, 2012, **23**, 785-795.
42. H. Tang, C. J. Murphy, B. Zhang, Y. Shen, E. A. Van Kirk, W. J. Murdoch and M. Radosz, *Biomaterials*, 2010, **31**, 7139-7149.
43. H. Han and M. E. Davis, *Molecular Pharmaceutics*, 2013, **10**, 2558-2567.
44. S. Yu, Y. Zhang, X. Wang, X. Zhen, Z. Zhang, W. Wu and X. Jiang, *Angewandte Chemie International Edition*, 2013, **52**, 7272-7277.
45. P. A. Faugeras, B. Boëns, P. H. Elchinger, F. Brouillette, D. Montplaisir, R. Zerrouki and R. Lucas, *European Journal of Organic Chemistry*, 2012, **2012**, 4087-4105.
46. H. Maeda, H. Nakamura and J. Fang, *Advanced Drug Delivery Reviews*, 2013, **65**, 71-79.
47. L. Zhou, R. Cheng, H. Tao, S. Ma, W. Guo, F. Meng, H. Liu, Z. Liu and Z. Zhong, *Biomacromolecules*, 2011, **12**, 1460-1467.

Graphical Abstract

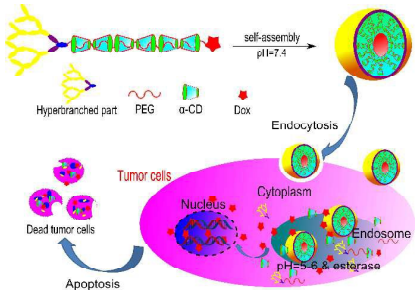

pH stimuli-responsive controlled selectively release drugs at endosomal compartments of the PR-g-DOX supramolecular micelles.